

Crystal Structure, Mössbauer Spectra, Thermal Expansion, and Phase Transition of Berthierite FeSb_2S_4

K. Łukaszewicz,^{*1} A. Pietraszko,^{*} J. Stępień-Damm,^{*} A. Kajokas,[†] J. Grigas,[†] and H. Drulis^{*}

^{*}Institute of Low Temperature and Structure Research, Polish Academy of Sciences, Okólna 2, 250-422 Wrocław, Poland; and [†]Department of Physics, University of Vilnius, Sauletekio al. 9/3, 2040 Vilnius, Lithuania

Received January 25, 2001; in revised form July 30, 2001; accepted August 9, 2001

Dielectric and ultrasound measurements of berthierite FeSb_2S_4 reported in the literature revealed a phase transition at $T_c = 348$ K. In the present study the phase transition was confirmed by Mössbauer spectra exhibiting anomalous behavior close to 350 K. Precise lattice parameters measured in the temperature region 305–380 K show a change of slope at about 350 K. The crystal structure of FeSb_2S_4 has been determined using single-crystal X-ray diffraction data at both room temperature and 370 K above the phase transition. The crystal structure is orthorhombic, $Z = 4$. At 295 K $a = 11.412(2)$ Å, $b = 3.763(1)$ Å, $c = 14.161(3)$ Å, and $R = 0.0280$, and at 370 K $a = 11.421(2)$ Å, $b = 3.771(1)$ Å, $c = 14.173(3)$ Å, and $R = 0.0274$. No symmetry change has been observed. At both temperatures the space group of FeSb_2S_4 is $Pnma$ with small changes in atomic parameters and interatomic distances. The transition observed at 348 K is, therefore, to be classified as a weak phase transition going on without essential changes in the crystal structure. © 2001 Academic Press

Key Words: FeSb_2S_4 ; berthierite; Mössbauer spectra; thermal expansion; crystal structure; weak phase transition.

INTRODUCTION

The crystal structure of berthierite FeSb_2S_4 at ambient temperature had been first determined and refined in the space group $Pnma$ in 1955 by Buerger and Hahn (1). New refinements (2, 3) confirmed previous results with small changes in structure parameters. The problem of the crystal structure and symmetry of berthierite remains nevertheless still open. Grigas and co-workers (4, 5) found that the crystal of FeSb_2S_4 was a semiconductor with both high electric conductivity and dielectric permittivity. Needle-shaped berthierite crystals show along the b axis (parallel to the needle axis) an anomalous dependence of permittivity and electric conductivity on temperature. A jump of both ϵ and $tg \delta$ has

¹To whom correspondence should be addressed. E-mail: kl@int.pan.wroc.pl.

been observed at 348 K. The phase transition of berthierite has been confirmed by the measurements of temperature dependence of attenuation of longitudinal ultrasound along the b axis (5). At microwaves the dielectric permittivity follows the Curie–Weiss law with the Curie temperature $T_c = 348$ K and the Curie–Weiss constant $C = 1.2 \times 10^3$ K (6).

The present study was aimed at explaining the nature of the phase transition observed in (4, 5) and checking the crystal structure of berthierite at both an ambient temperature and 370 K, well above the expected phase transition temperature.

EXPERIMENTAL

Data were collected at ambient temperature $T = 295$ K and at $T = 370$ K by the KUMA-Diffraction KM4 diffractometer with graphite-monochromated $\text{MoK}\alpha$ radiation ($\lambda = 0.71073$ Å). Precise lattice parameters were determined as a function of temperature by the Bond method (7) developed in our laboratory for precise measurements of the thermal expansion of single crystals (8). Intensities were measured with the ω/θ scan technique with a scan speed depending on intensity. No significant intensity variation was observed for two standard reflections. The reflection intensities were corrected for the Lorentz and polarization effects. Empirical absorption correction was applied based on Ψ scans for selected reflections. The extinction correction was introduced in the full-matrix least-squares refinement on F^2 performed by using the SHELXL-97 program (9). Preliminary atomic positions were taken from (3).

The ^{57}Fe Mössbauer spectra were taken at several temperatures in the range of 295–385 K with a conventional constant acceleration spectrometer. The source was ^{57}Co in an Rh matrix. The velocity scale calibration and the isomer shift values estimation have been performed relative to $\text{Na}_2(\text{NO})\text{Fe}(\text{CN})_5 \cdot 2\text{H}_2\text{O}$.

Crystal data and details of the refinement procedure are presented in Table 1. Weighted R factors wR_2 and goodness



TABLE 1
Crystal Structure Determination Data for Berthierite
FeSb₂S₄ at 295 and 370 K

Chemical formula weight	427.59	
Z	4	
F(000)	768	
Wavelength, MoK α (Å)	0.71073	
Crystal system	Orthorhombic	
Crystal shape and size	Needles, approximately 0.24 × 0.03 × 0.03 mm	
Absorption correction	Ψ scan	
Data collection: KUMA-Diffraction KM-4 diffractometer, ω/θ scan with pre-scanning		
θ range for data collection (°)	2–30	
Reflections 303 and 02 $\bar{3}$ monitored every 50 reflections, intensity variation < 1%		
Unit cell dimensions from independent thermal expansion measurements:		
Temperature (K)	295	370
<i>a</i> (Å)	11.412(2)	11.421(2)
<i>b</i> (Å)	3.763(1)	3.771(1)
<i>c</i> (Å)	14.161(3)	14.173(3)
<i>V</i> (Å ³)	608.1(2)	610.4(2)
Density <i>D_x</i> (mg/m)	4.670	4.653
Absorption coefficient (mm ⁻¹)	12.404	12.358
Space group	<i>Pnma</i>	<i>Pnma</i>
Index ranges: <i>h</i>	–16 → 16	–16 → 16
<i>k</i>	–5 → 0	–3 → 5
<i>l</i>	–19 → 19	–13 → 19
Measured reflections	3483	2343
Independent reflections, total	998	955
<i>R_{int}</i>	0.0358	0.0295
Observed reflections [<i>I</i> > 2 σ (<i>I</i>)]	886	882
Extinction coefficient	0.0027	0.0023
Number of parameters	44	44
<i>R₁</i> [<i>I</i> > 2 σ (<i>I</i>)]	0.0280	0.0274
<i>wR₂</i> (<i>F</i> ²) [<i>I</i> > 2 σ (<i>I</i>)]	0.0597	0.0640
(Δ/σ) _{max}	< 0.001	< 0.001
$\Delta\rho_{\text{max}}/\Delta\rho_{\text{min}}$ (e Å ⁻³)	1.34/–1.21	1.8/–1.8
$\Delta\rho_{\text{max}}$ at	0.66 Å from Sb1	0.81 Å from Sb2

of fit *S* are based on F^2 and conventional R_1 factor based on F_0 , with F_0 set to zero for negative F_0^2 .

RESULTS AND DISCUSSION

Mössbauer spectra at RT and 378 K are presented in Fig. 1. The hyperfine parameters, the quadrupole splitting, *QS*, and the isomer shift, *IS*, have been calculated by the least-squares fits of the experimental results within the Lorentz approximation for one doublet coming from the studied sample and another one from the furnace holder. In spite of this, the parameters estimated at 295 K are in good agreement with those reported in earlier Mössbauer studies (10) where only one quadrupole doublet had been observed (there were no impurity subspectra).

The temperature dependencies of *QS* and *IS* of the Fe nucleus are shown in Fig. 2. Both parameters exhibit anomalous behaviors at temperatures close to 350 K. Such

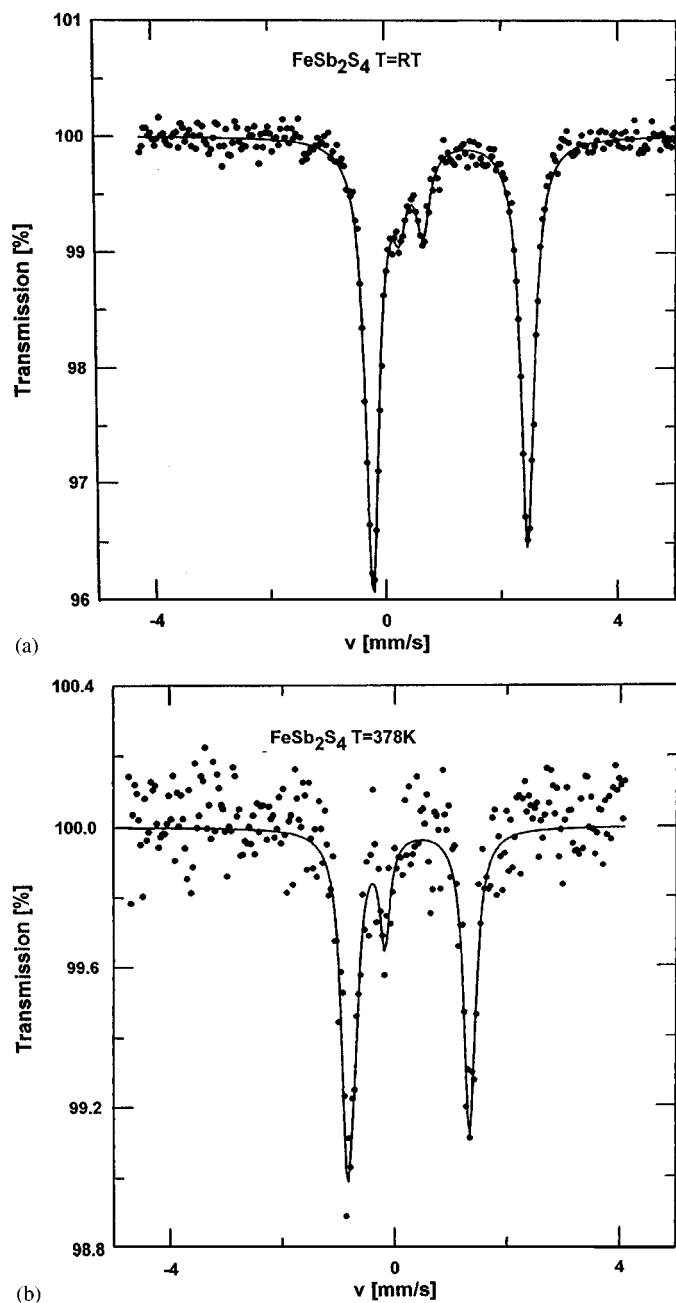


FIG. 1. The Mössbauer spectra of FeSb₂S₄ at temperatures (a) 295 K and (b) 378 K. A small doublet visible in the central part of the spectra comes from the furnace holder.

changes in the *QS* and *IS* parameters are usually observed when the material undergoes the phase transition induced by the temperature or by the pressure. From the Mössbauer data it appears that the FeSb₂S₄ undergoes apparently in the temperature range 323–365 K a structural phase transition of second order. Nevertheless, we cannot confirm the symmetry change connected with the phase transition at 348 K as suggested in (4). In such a case, in the phase of

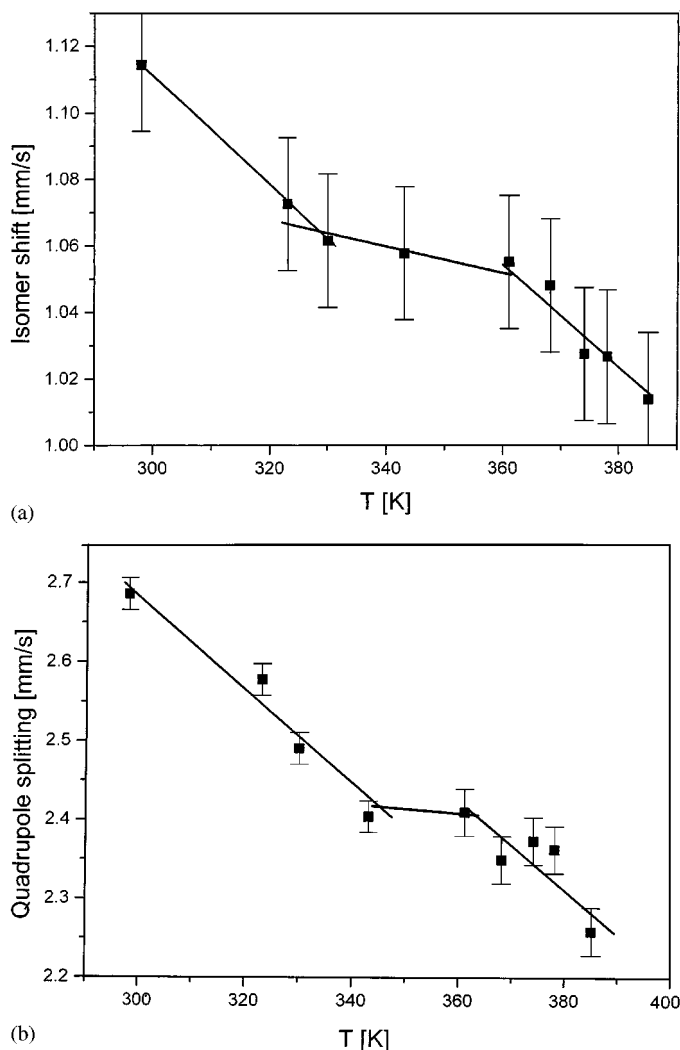


FIG. 2. (a) The isomer shift and (b) the quadrupole splitting of ^{57}Fe Mössbauer spectra of FeSb_2S_4 as a function of temperature.

lower symmetry we would observe two superimposed doublets in Mössbauer spectra connected with two nonequivalent Fe atoms. The attempts, however, to analyze the Mössbauer spectra with two doublets have failed. A narrow line with almost the same linewidth ($\Gamma = 0.28$ mm/s) at both room temperature and 378 K justifies the description of Mössbauer spectra with a single quadrupole doublet. In the frame of our experimental accuracy it appears that the phase transition observed in FeSb_2S_4 at 348 K is isostructural with no symmetry change.

Figure 3 shows lattice parameters and lattice volume of FeSb_2S_4 as a function of temperature. Each parameter exhibits a small change in slope at about 350 K manifested as an anomaly of thermal expansion, indicating weak phase transition of second order. The crystal structure of FeSb_2S_4 at both room temperature and 370 K was refined in the

TABLE 2
Atomic Coordinates and Equivalent Isotropic Displacement Parameters U_{eq} for FeSb_2S_4

Atom	Site	x	y	z	U_{eq}
$T = 295$ K					
Fe	4c	0.31673(6)	0.25	0.66495(5)	0.0164(2)
Sb1	4c	0.14473(3)	0.25	0.93684(2)	0.0177(1)
Sb2	4c	0.03882(3)	0.25	0.38563(2)	0.0144(1)
S1	4c	0.8045(1)	0.25	0.27030(8)	0.0150(2)
S2	4c	0.4220(1)	0.25	0.81593(9)	0.0164(2)
S3	4c	0.2234(1)	0.25	0.50584(9)	0.0152(2)
S4	4c	0.5494(1)	0.25	0.40456(8)	0.0150(2)
$T = 370$ K					
Fe	4c	0.31639(7)	0.25	0.66506(6)	0.0207(2)
Sb1	4c	0.14453(3)	0.25	0.93692(3)	0.0219(1)
Sb2	4c	0.96087(3)	0.25	0.38547(3)	0.0178(1)
S1	4c	0.8042(1)	0.25	0.2700(1)	0.0187(3)
S2	4c	0.4226(1)	0.25	0.8160(1)	0.0205(3)
S3	4c	0.2235(1)	0.25	0.5060(1)	0.0191(3)
S4	4c	0.5491(1)	0.25	0.4046(1)	0.0177(3)

centrosymmetric space group $Pnma$ and in four orthorhombic subgroups of $Pnma$: $P2_12_12_1$, $Pmn2_1$, $Pna2_1$, and $Pmc2_1$. In all cases the discrepancy indices R were satisfactory. There is no reason, therefore, to assume the polar space group, though in the high-temperature phase slightly better agreement between F_o and F_c was obtained for the space group $Pmn2_1$. Atomic parameters for FeSb_2S_4 at both temperatures are listed in Table 2.

Figure 4 shows a perspective view of FeSb_2S_4 along $[010]$. The three-dimensional framework consists of two polyhedral types: $[\text{FeS}_6]$ octahedra and $[\text{SbS}_5]$ orthorhombic pyramids. Bond distances and angles for the polyhedra are listed in Table 3. By sharing two opposite edges, Fe octahedra form infinite chains $(\text{FeS}_4)_n^{6n-}$ running parallel to the $[010]$ axis. The Sb^{3+} cations are inserted between the chains inside an orthorhombic pyramid (Fig. 5). Both Figs. 4 and 5 were prepared by using the program in (11). The Sb1 cations are attached to $(\text{FeS}_4)_n^{6n-}$ chains by short Sb1–S3 and Sb1–S4 bonds. The chains joined by Sb2 form layers perpendicular to $[001]$. It is worth noting a slight external shift of the Sb1 position in relation to the base of the pyramid, whereas Sb2 remains in the plane of the base of the pyramid.

In semiconductors with a great amount of covalency, such as berthierite, the electronic subsystem plays an important role in a delicate balance of short- and long-range interactions (6). One can assume that even the small changes in the lattice significantly disturb the electronic subsystem, inducing spontaneous polarization and the anomalies of semiconductive and dielectric properties. It appears, therefore, that the observed phase transition in FeSb_2S_4 semiconductor is mostly related to the electronic subsystem.

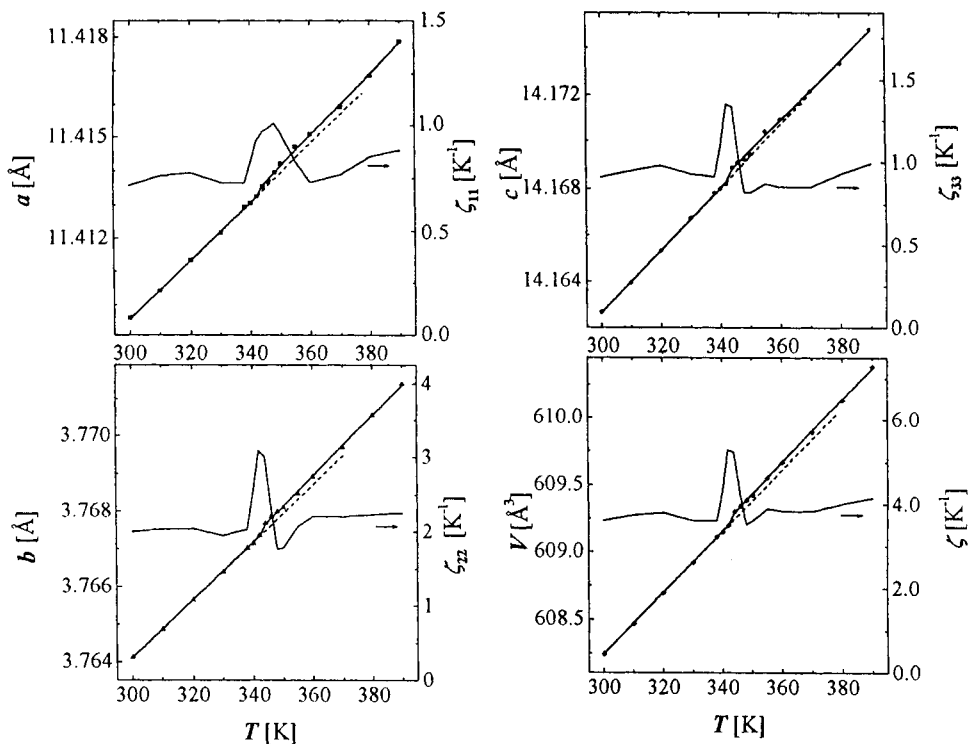


FIG. 3. Lattice parameters a , b , and c and lattice volume V of FeSb_2S_4 as a function of temperature. Superimposed second derivatives indicate a change in slope.

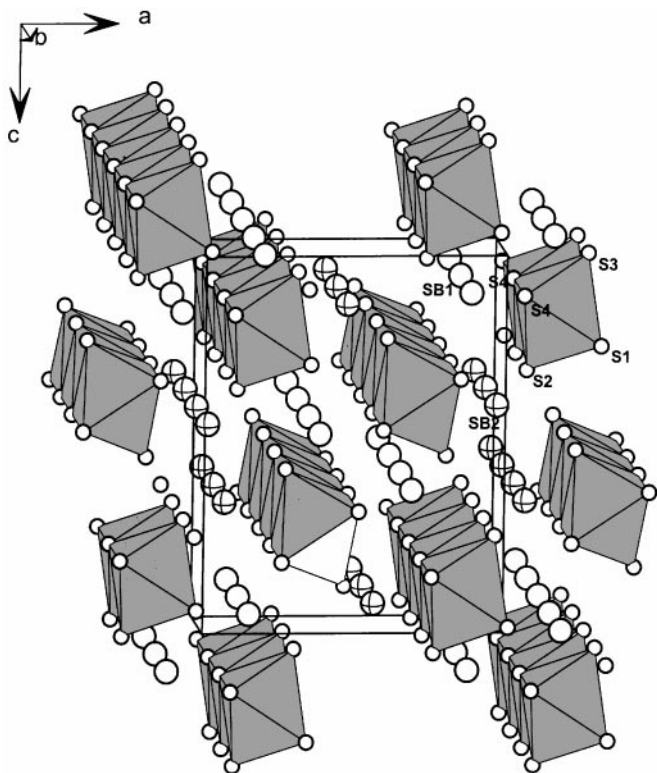


FIG. 4. Perspective view of the crystal structure of FeSb_2S_4 along $[010]$ with $[\text{FeS}_6]$ octahedra.

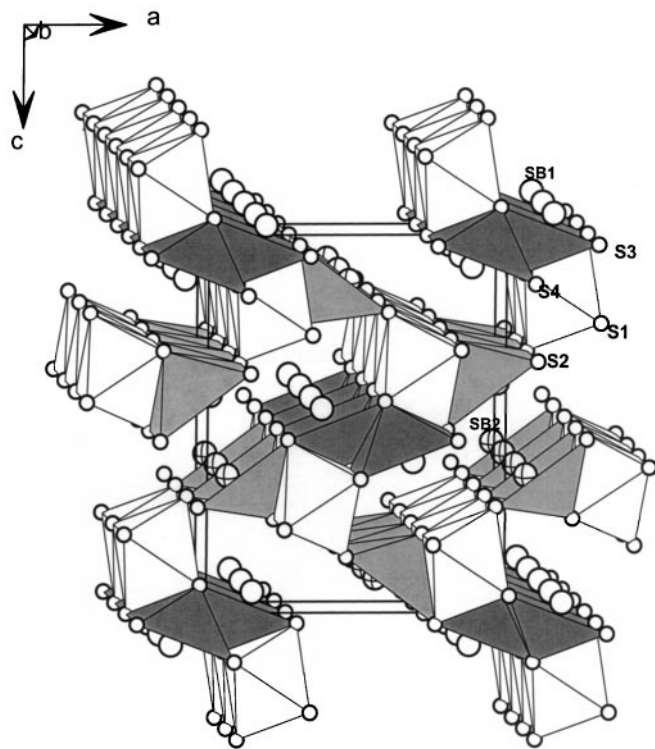


FIG. 5. Perspective view of the crystal structure of FeSb_2S_4 along $[010]$ with $[\text{SbS}_5]$ pyramids.

TABLE 3
Main Interatomic Distances (Å) and Angles (°) in FeSb₂S₄

Fe	S2	S3	S1	S1	S4	S4
$T = 295 \text{ K}$						
Fe octahedron, site symmetry: m						
S2	2.453(2)	4.942(2)	3.422(1)	3.422(1)	3.660(2)	3.660(2)
S3	175.97(4)	2.492(2)	3.700(2)	3.700(2)	3.446(1)	3.446(2)
S1	87.22(4)	94.44(4)	2.509(2)	3.763(1)	3.477(2)	5.123(1)
S1	87.22(4)	95.44(4)	97.18(4)	2.509(2)	5.123(1)	3.477(2)
S4	92.40(4)	84.81(3)	85.42(3)	177.35(4)	2.616(1)	3.763(1)
S4	92.40(4)	84.81(3)	177.35(4)	85.42(3)	91.97(3)	2.616(1)
$\langle \text{Fe-S} \rangle = 2.533 \text{ \AA}$						
Sb1 pyramid			Sb2 pyramid			
Sb1-S4	2.496(1)		Sb2-S1		2.422(1)	
Sb1-S3	2.600(1)		Sb2-S2		2.508(1)	
Sb1-S4	2.600(1)		Sb2-S1		2.508(1)	
Sb1-S4	2.942(1)		Sb2-S1		3.215(1)	
Sb1-S4	2.942(1)		Sb2-S1		3.215(1)	
$\langle \text{Sb-S} \rangle = 2.716 \text{ \AA}$			$\langle \text{Sb-S} \rangle = 2.774 \text{ \AA}$			
$T = 370 \text{ K}$						
Fe octahedron, site symmetry: m						
Fe	S2	S3	S1	S1	S4	S4
S2	2.458(2)	4.946(2)	3.687(1)	3.687(1)	3.665(2)	3.665(2)
S3	175.65(64)	2.491(2)	3.706(2)	3.706(2)	3.450(1)	3.450(2)
S1	87.24(4)	95.62(4)	2.510(2)	3.771(2)	3.482(2)	5.133(1)
S1	87.24(4)	95.62(4)	97.40(6)	2.510(2)	5.133(1)	3.384(2)
S4	92.21(4)	84.76(4)	85.38(3)	177.14(4)	2.625(2)	3.771(2)
S4	92.21(4)	84.76(3)	177.14(4)	85.38(3)	91.84(3)	2.625(1)
$\langle \text{Fe-S} \rangle = 2.537 \text{ \AA}$						
Sb1 pyramid			Sb2 pyramid			
Sb1-S4	2.496(2)		Sb2-S1		2.425(1)	
Sb1-S3	2.605(1)		Sb2-S2		2.510(1)	
Sb1-S4	2.605(1)		Sb2-S1		2.510(1)	
Sb1-S4	2.942(1)		Sb2-S1		3.218(1)	
Sb1-S4	2.942(1)		Sb2-S1		3.218(1)	
$\langle \text{Sb-S} \rangle = 2.718 \text{ \AA}$			$\langle \text{Sb-S} \rangle = 2.776 \text{ \AA}$			

Supplementary data including anisotropic temperature factors and lists of structure factors may be obtained upon request from the authors.

ACKNOWLEDGMENT

The authors are indebted to Mr. P. Gaczyński for performing Mössbauer measurements.

REFERENCES

1. M. J. Buerger and T. Hahn, *Am. Mineral.* **40**, 226 (1955).
2. K. Bente and A. Edenharter, *Z. Kristallogr.* **187**, 31 (1989).
3. P. Lemoine, D. Carre, and F. Robert, *Acta Crystallogr. C* **47**, 938 (1991).
4. J. Grigas, A. Orliukas, and N. N. Mozgova, *Lietuvos Fiz. Rinkinys* **15**, 872 (1975).
5. J. Grigas, *Ferroelectrics* **20**, 173 (1978).
6. J. Grigas, "Microwave Dielectric Spectroscopy of Ferroelectrics and Related Materials." Gordon & Breach, New York, 1996.
7. W. L. Bond, *Acta Crystallogr.* **13**, 814 (1960).
8. D. Kucharczyk, A. Pietraszko, and K. Łukaszewicz, *J. Appl. Crystallogr.* **26**, 467 (1993).
9. G. M. Sheldrick, SHELXL-97: A Program for Crystal Structure Refinement, Univ. of Goettingen, Germany, 1997.
10. P. Bonville, C. Garcin, A. Gérard, P. Imbert, and M. Wintenberger, *Hyperfine Interaction* **52**, 279 (1989).
11. K. Brandenburg, Diamond Version 2.1d, Crystal Impact GbR, Created Nov 16, 2000, Serial no. 9-48100.